

Geometric Characterization of Many Body Localization

W. N. Faugno, Tomoki Ozawa

Advanced Institute for Materials Research (WPI-AIMR), Tohoku University, Sendai 980-8577, Japan

(Dated: October 14, 2024)

Many body localization (MBL) represents a unique physical phenomenon, providing a testing ground for exploring thermalization, or more precisely its failure. Here we characterize the MBL phase geometrically by the many-body quantum metric (MBQM), defined in the parameter space of twist boundary. We find that we can characterise the transition by comparing the thermodynamic limits of the MBQM and localization length as defined in the modern theory of polarization and insulators. As such we find that we can extract a natural localization length in the MBL phase that relies only on the real space spread of the wave function and can be measured through lattice shaking or AC response measurements.

Advancements in highly controllable experimental platforms, such as optical lattices[1–4], trapped ions[5], and Rydberg atom arrays[6, 7], have allowed for realizations of well isolated quantum systems in the lab where quantum dynamics and non equilibrium physics can be observed [8, 9]. Of particular interest are nonergodic systems, which do not thermalize within a finite time. These systems can host stable phases of matter and help to understand thermalization mechanisms [10]. Thus far the only known robust nonergodic phase is many body localization (MBL), which arises from the interplay of disorder and interactions [11, 12]. In contrast, other nonergodic phases, such as non-interacting phases, quantum scars or integrable models, typically thermalize with the addition of some perturbation [13].

Anderson localization was the first identified nonergodic system wherein disorder in a non-interacting system localizes all eigenstates [14]. Following studies saw the inclusion of interactions to determine the stability of the ground state in this localized phase, finding that indeed localization persisted in several regimes [15–17]. More recent studies have found that excited states, even those corresponding to infinite temperature, can remain localized, resulting in a phenomenon termed MBL [18–20].

MBL hosts many interesting properties beyond those observed in its non-interacting counterpart and demonstrates a unique dynamical phase transition between the localized and delocalized regions. The phase boundary can be determined through the entanglement entropy scaling with system size, growing with volume in the delocalized phase and following an area law in the localized phase [21]. Additionally the entanglement entropy of initial product states has been shown to grow logarithmically, in contrast to the quickly saturating entanglement entropy in non-interacting Anderson insulators [22, 23]. The unique behavior of the entanglement entropy is related to the localization in Fock space in addition to real space localization. This has been shown to be related to the emergence of a set of quasilocal integrals of motion (LIOM), which has allowed for the construction of phenomenological models of MBL[24]. Strong evidence

of MBL has been found in the disordered Bose-Hubbard [25, 26] and Fermi-Hubbard models [27] in 1D as well as quasi-disordered lattice systems with non commensurate periodic external potentials [28].

An important parameter in understanding insulating states is the characteristic localization length. To present, there have been several proposed approaches to extracting the localization length in MBL systems. For example, a localization length can be defined in terms of the inverse participation ratio obtained from the single particle density matrix [29]. Other methods rely on phenomenological models constructed from the extensive set of LIOM, which introduces a hierarchy of length scales[30, 31]. The LIOM have been constructed explicitly for the XXZ model [32], the disordered hardcore Fermi-Hubbard model [33, 34], and the Heisenberg model[35]. Although there are several different localization lengths that appear in MBL, their physical meaning or experimental signature is often unclear.

A natural localization length has been defined in the modern theory of insulators, built upon the theory of polarization[36–43]. This localization length allows us to distinguish conducting and insulating phases as it diverges in the former, but remains finite in the latter. Additionally, for insulators, this localization length can be related to the so-called quantum metric, which defines the distance between wave functions in the space of some parameter of the Hamiltonian. Typical choices of such parameters are the crystal momentum or the twist boundary phase. This formalism has been applied in several paradigmatic contexts, including quantum Hall insulators[44], Mott insulators[45], and Chern insulators[46]. Twist boundary condition was used to characterize the MBL phase through the Drude weight [47], which also captures the metal-insulator transition. From a more general perspective, the MBQM is a particular form of the fidelity susceptibility, which has been used to characterize the MBL through level spacings from their connection to random matrix theory [48–50].

In this work, we demonstrate that this natural characteristic length scale for localization in real space can be used to characterise the ergodic-MBL phase transi-

tion by comparing it with the MBQM. We apply this method to the disordered hardcore Bose-Hubbard chain at half-filling. We find that in the MBL phase the thermodynamic limit of both the localization length and the MBQM agree, but the quantities are unrelated in the ergodic phase. In the MBL phase, we are able to extract a characteristic localization length from the thermodynamic limit of the MBQM.

We review the definitions of the localization length in PBC and the many body quantum metric (MBQM), the two key quantities in this work. The localization length of a many-body state Ψ is built on the quantity

$$D_N = -N \ln |z_N|^2 \quad (1)$$

$$z_N = \langle \Psi | e^{2i\pi X_{CM}/L} | \Psi \rangle \quad (2)$$

where N is the number of particles, $X_{CM} \equiv \sum_n x_n$ with x_n the position operator for the n -th particle, and L is the length of the system. The quantity z_N defines both localization and polarization properties of systems with PBC where the position operator is ill-defined. In particular, localization properties are captured by the thermodynamic limit of $D_\infty = \lim_{N \rightarrow \infty} D_N$, which has been shown to discriminate between insulators and conductors: it remains finite in the former, but diverges in the latter with system size [36, 51]. This property is known to hold for both band and disorder induced insulators and for both interacting and non-interacting systems. For an insulator, we define the localization length $\ell = \sqrt{D_\infty}/2\pi n$ where n is the density [52]. Thus, this quantity provides a general theoretical framework for probing conduction properties and defining a natural localization length.

The quantity D_∞ defined above is proportional to the many-body quantum metric in the thermodynamic limit. The MBQM is a geometrical property of many-body quantum states, here defined in the parameter space of twisted boundary conditions. We consider one-dimensional systems in this article where the MBQM is equivalent to the quantum geometric tensor. Twisted boundary conditions with phase θ are equivalent to inserting a flux θ through the system with the wavefunction obeying the standard periodic boundary condition (PBC) without twist [53]. Let us denote the Hamiltonian of the system with a flux θ inserted by $H(\theta)$. The MBQM, which we denote by $g(\phi_0, \theta)$, for a state $|\phi_0\rangle$, can then be defined in two equivalent ways [54, 55]

$$g(\phi_0, \theta) = \langle \partial_\theta \phi_0(\theta) | \partial_\theta \phi_0(\theta) \rangle - |\langle \phi_0(\theta) | \partial_\theta \phi_0(\theta) \rangle|^2 \quad (3)$$

$$g(\phi_0, \theta) = \sum_{n \neq 0} \frac{\langle \phi_0 | \partial_\theta H(\theta) | \phi_n \rangle \langle \phi_n | \partial_\theta H(\theta) | \phi_0 \rangle}{(E_0 - E_n)^2}, \quad (4)$$

where the sum is over all the eigenstates $|\phi_n\rangle$, whose corresponding eigenenergies are E_n , different from the state under consideration, $|\phi_0\rangle$. (In general, both $|\phi_n\rangle$ and E_n depend on θ .) When the system is large enough, we can

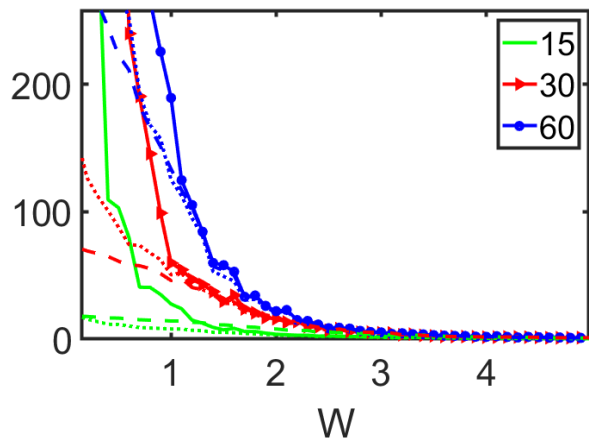


FIG. 1. Quantum Metric L^2g (solid), variance (dashed) and $(L/2\pi)^2 D_1$ (dotted) as a function of disorder strength W for a single particle Anderson Insulator system. These quantities are all equivalent a localized state. The discrepancy at low disorder arises from the localization length becoming comparable to the system size.

expect that $g(\phi_0, \theta)$ does not depend on θ following arguments similar to those in Refs. [38, 53, 56]; we will thus consider MBQM at $\theta = 0$ in the following discussion without loss of generality. To simplify notation we will suppress the arguments. When the wavefunction is fully localized within a finite region, one can show that $g = \text{Var}(X_{CM})/L^2$ for a system with length L [38].

As stated earlier, the MBQM and the quantity D_N are related in the thermodynamic limit for insulators [52]. The precise relation is given by

$$D_\infty = g_\infty = \lim_{N \rightarrow \infty} g_N = \lim_{N \rightarrow \infty} 4\pi^2 N g \quad (5)$$

where we have defined g_N as the MBQM with appropriate prefactors and label the thermodynamic limit as g_∞ . Thus, the localization length of an insulator can also be defined by the MBQM as $\ell = \sqrt{g_\infty}/2\pi n$ [37].

We apply this method to the disordered hardcore Bose-Hubbard chain to demonstrate that it indeed captures the transition from the ergodic phase to the MBL phase. The Hamiltonian is written as

$$H = \sum_j -t(a_{j+1}^\dagger a_j + a_j^\dagger a_{j+1}) + U_\infty n_j n_j + U n_{j+1} n_j + \mu_j n_j \quad (6)$$

where a_j^\dagger, a_j are the bosonic creation and annihilation operators on site j , $n_j = a_j^\dagger a_j$ is the density operator, t is the hopping parameter, $U_\infty \rightarrow \infty$ imposes the hardcore constraint, U is the nearest neighbor interaction strength, and μ_j is the disordered chemical potential on site j taken from the uniform distribution $[-W, W]$. We fix $t = 1$ throughout the calculations presented below. This model is known to exhibit a dome like phase boundary

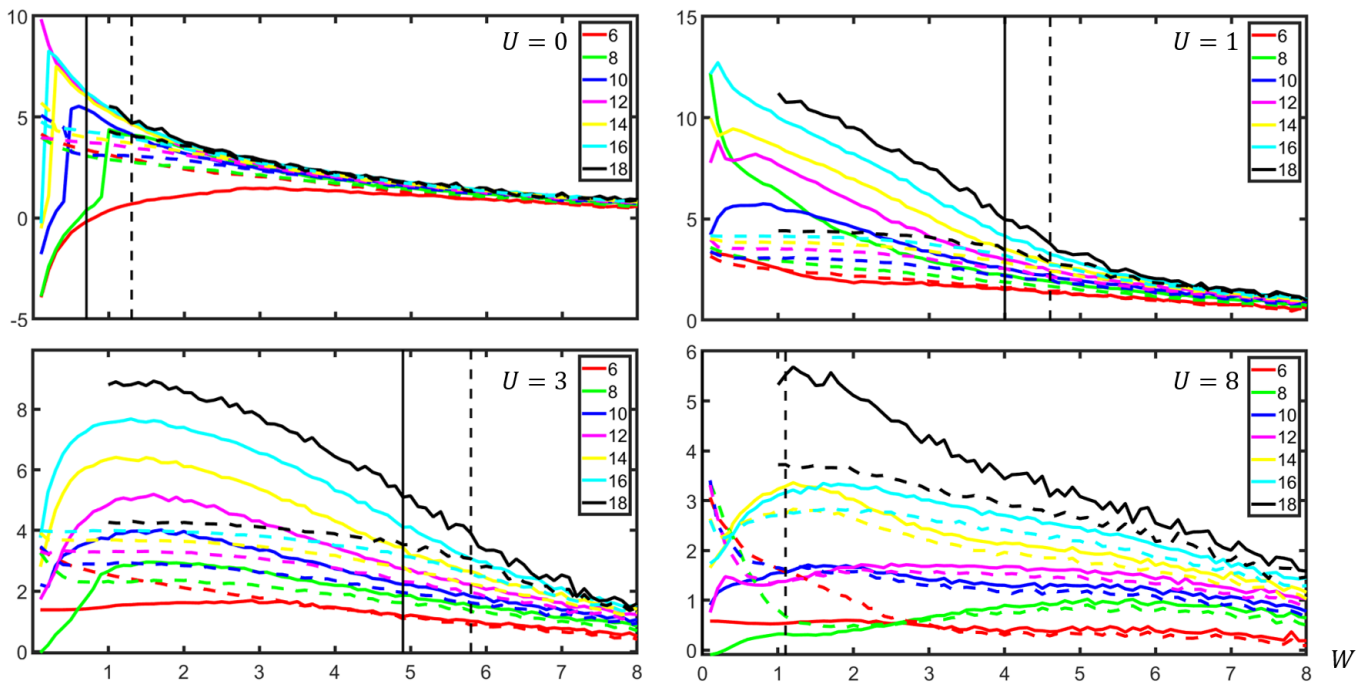


FIG. 2. Quantum metric $g_N = 4\pi^2 N g$ (solid) and localization length parameter $D_N = -N \ln |z_N|^2$ (dashed) versus disorder strength for different fixed interaction strengths U . The legend refers to the number of lattice sites in the chain L . Vertical solid and dashed lines correspond to contours presented on the phase diagram Fig. 3.

between the ergodic and MBL phases as a function of U and W [27, 57].

Before considering the many-body system, we demonstrate that this theoretical framework captures the localization properties of the single particle Anderson insulator, setting $U = 0$ in Eq. 6. We calculate the MBQM and D_N of the eigenstate in the middle of the energy spectrum, taking the median over 100 disorder realizations for systems sizes ranging from $L = 15$ to 60 for disorder parameter W from 0.1 to 8. (We take the median as we find it converges more quickly than the average.) A disordered single particle system is expected to be an insulator for any disorder strength and thus we do not expect any metal-insulator transition. We present the values of $L^2 g$ (solid), $(L/2\pi)^2 D_1$ (dotted), and $\text{Var}(X)$ (dashed) as a function of disorder W in Fig. 1. The variance is calculated by shifting the localized state away from the boundary and calculating as though it were an open boundary system where the typical definition of variance is well defined. Note that for large disorder, all quantities agree as is expected. For low disorder, discrepancies arise due to finite size effects since the localization length of the state becomes larger than the finite system. Evidence of this is seen in how the agreement improves at lower disorder strengths as the system size increases.

Now we consider the many-body problem. We will calculate the MBQM and D_N at half-filling for a range of interaction and disorder strengths at system lengths from $L = 6$ to 18. We take the median over 1000 dis-

order realizations, except for the largest system $L = 18$ where we are limited to 120 realizations by computation constraints. We take the eigenstate from the center of the spectrum as this corresponds to the infinite temperature state. As in the single particle system, we consider the median as the mean converges slowly due to accidental near degeneracies. Due to memory constraints we implement an algorithm for calculation of the quantum metric that does not require full diagonalization of the Hamiltonian. Details of the algorithm are provided in the supplement. For the largest system, we are unable to obtain values when $W < 1$.

We present the values of g_N (solid) and D_N (dashed) for each system size as a function of W for four different values of U in Fig. 2. For the non-interacting case, the quantities agree for large disorder strength. The discrepancies at low disorder can be attributed to finite size effects. When the interaction is turned on we observe that the quantities tend to the same value for large disorder regardless of system size, but the two values are no longer related at low disorder with a strong system size dependence. This apparent difference in behavior suggests the existence of the ergodic-MBL phase transition, but to truly establish the transition, we must compare the thermodynamic limits.

To determine the phase boundary, we take the thermodynamic limit by fitting both g_N and D_N with an exponential $Ae^{B/L}$ where A and B are fitting parameters and L is the system length. Examples of the fitting are

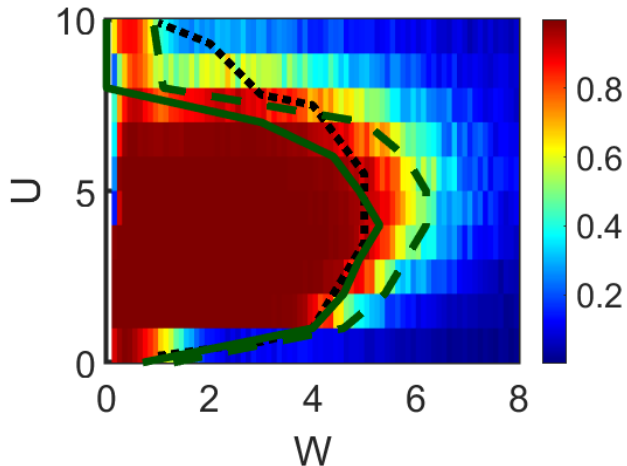


FIG. 3. Phase Diagram of the ergodic-MBL transition obtained from $\Delta = |g_\infty - D_\infty|/(g_\infty + D_\infty)$. This quantity is approximately 1 in the ergodic regime and goes to 0 in the MBL phase. We mark a previously obtained phase boundary from Ref. [27] in black and the contours of $\Delta = 0.9$ (dashed) and 0.5 (solid) in green.

provided in the supplement, but we note that the phase boundary is insensitive to the choice of fitting function. The fitting only captures a true divergence when A becomes infinite. As such we do not expect the fitting to be accurate in the ergodic regime. Indeed the error bars in the both g_∞ and D_∞ become large as the disorder decreases. We observe that the MBQM diverges strongly with system size while the fate of D_N in the thermodynamic limit is ambiguous. Previous calculations of D_N demonstrate the difficulty in capturing its divergent nature from finite size calculations [37, 42, 43]. As such we compare the thermodynamic limits to define our phase boundary.

From the thermodynamic limits we define the quantity $\Delta = |D_\infty - g_\infty|/(D_\infty + g_\infty)$, which should go to zero in the MBL phase where the thermodynamic limits agree and go to some finite value in the ergodic phase where the quantities are no longer related. We have plotted the value of this parameter as a function of U and W in Fig. 3. (The same data is presented in the supplement as plots at constant U .) We find there is a striking transition as the disorder increases resulting in a dome-shaped phase boundary. In the region where the system is ergodic, Δ tends to 1, showing that the two quantities, though both divergent, behave differently when taking their thermodynamic limits. We mark in dark green dashed and solid lines the contour where the value of Δ drops below 0.5 and 0.9. The dotted black line corresponds to a previously calculated phase diagram from the dynamical exponents [27], demonstrating that our method agrees with previous characterizations of the transition. From this parameter, we see that the MBL

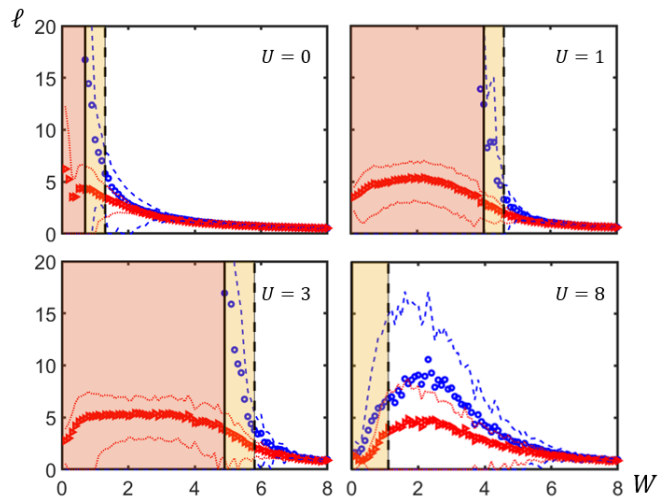


FIG. 4. Localization as a function of disorder for different interaction strengths. Localization lengths are extracted from the thermodynamic limits g_∞ (blue circle) and D_∞ (red). Thin lines show the error in the thermodynamic limits from the fitting. The solid and dashed vertical lines correspond to the phase boundaries reported in Fig. 3. The shaded regions denote where the system is ergodic (red) and transitional (yellow) and the MBQM no longer coincides with D_∞ .

phase is stabilized for very large disorder regardless of the interaction strength and even captures the re-entrant behavior for fixed disorder where MBL can occur for large and small interactions [58–60].

Once we have established that we are in the MBL phase by the agreement between the two quantities in the thermodynamic limit, we can define a localization length as $\ell = \sqrt{D_\infty}/2\pi n$, or equivalently $\ell = \sqrt{g_\infty}/2\pi n$ as proposed in Ref. [36]. We present the extracted localization lengths from the quantum metric (blue circles) and localization parameter D (red triangles) in Fig. 4 as a function of disorder strength W for different fixed interaction strengths U . (Localization lengths for the full phase diagram are provided in the supplement.) The vertical solid and dashed lines mark the corresponding phase boundaries from Fig. 3. The thermodynamic limits of both quantities tend to agree within reasonable error bars (dashed lines) when the system is within the MBL phase. In the red shaded region, the system is ergodic and we expect that the localization length is divergent. We observe this in the MBQM, but as stated earlier the divergent behavior of D_N is not apparent yet for the accessible system sizes.

The quantum metric and localization length provide an excellent method for characterizing the ergodic-MBL transition. Considering both quantities together allows us to overcome the difficulty in determining whether the quantity D_N is truly divergent or simply large. Our calculation demonstrates that the MBL transition in this system can be considered a proper metal-insulator tran-

sition and can be captured by the same theoretical machinery as in band conductors and Anderson insulators. The localization length presented above is exactly that used in more conventional insulating phases relying only on the real space spread of the center of mass. This length scale can be interpreted as a single particle spread through the relation $L^2 g = \text{Var}(X_{CM})$, which in terms of our localization length suggests $\ell^2 \approx \text{Var}(X_{CM})/N$. This is in contrast to previous localization lengths in MBL that rely on Fock space localization.

The MBQM offers insight into further understanding the MBL phase. Experimentally it has been proposed that the MBQM can be extracted from the participation ratio in a lattice shaking experiment [61]. The MBQM should allow for a straightforward and general method for detecting the presence of MBL in a variety of systems, including fermionic and spin systems as well as systems without disorder. Our method relies on the fact that the ergodic-MBL transition is also a metal-insulator transition. We do not expect our method to detect ergodic-MBL transitions that may occur at insulator-insulator transitions, an example of which has recently been reported [62]. The definition of the localization length is still applicable despite the inability to detect the phase transition. Moving beyond exact diagonalization methods to calculate the MBQM for larger systems will allow for improved accuracy in determining the phase boundary. Additionally, it remains to be seen how the MBQM compares with previously proposed localization lengths, but we note it is of the same order as the IPR reported in [29]. In higher dimensions, the MBQM has a tensorial structure reflecting the localization of many-body quantum systems in different directions; such a higher dimensional MBQM may be able to determine the fate of MBL in higher dimensions.

ACKNOWLEDGEMENTS

We thank Ryusuke Hamazaki and Henning Schomerus for discussions on many-body localization. This work has been supported by JSPS KAKENHI Grant Number JP20H01845, JST PRESTO Grant No. JPMJPR2353, JST CREST Grant Number JPMJCR19T1.

-
- [1] I. Bloch, J. Dalibard, and W. Zwerger, Many-body physics with ultracold gases, *Rev. Mod. Phys.* **80**, 885 (2008).
- [2] V. Bilokon, E. Bilokon, M. C. Bañuls, A. Cichy, and A. Sotnikov, Many-body correlations in one-dimensional optical lattices with alkaline-earth(-like) atoms, *Scientific Reports* **13**, 10.1038/s41598-023-37077-1 (2023).
- [3] L. Chomaz, I. Ferrier-Barbut, F. Ferlaino, B. Laburthe-Tolra, B. L. Lev, and T. Pfau, Dipolar physics: a review of experiments with magnetic quantum gases, *Reports on Progress in Physics* **86**, 026401 (2022).
- [4] D. Malz and J. I. Cirac, Few-body analog quantum simulation with rydberg-dressed atoms in optical lattices, *PRX Quantum* **4**, 020301 (2023).
- [5] R. Blatt and C. F. Roos, Quantum simulations with trapped ions, *Nature Physics* **8**, 10.1038/nphys2252 (2012).
- [6] C. S. Adams, J. D. Pritchard, and J. P. Shaffer, Rydberg atom quantum technologies, *Journal of Physics B: Atomic, Molecular and Optical Physics* **53**, 012002 (2019).
- [7] X. Wu, X. Liang, Y. Tian, F. Yang, C. Chen, Y.-C. Liu, M. K. Tey, and L. You, A concise review of rydberg atom based quantum computation and quantum simulation*, *Chinese Physics B* **30**, 020305 (2021).
- [8] T. Kinoshita, T. Wenger, and D. S. Weiss, A quantum newton's cradle, *Nature* **440**, 10.1038/nature04693 (2006).
- [9] R. Vasseur and J. E. Moore, Nonequilibrium quantum dynamics and transport: from integrability to many-body localization, *Journal of Statistical Mechanics: Theory and Experiment* **2016**, 064010 (2016).
- [10] R. Nandkishore and D. A. Huse, Many-body localization and thermalization in quantum statistical mechanics, *Annual Review of Condensed Matter Physics* **6**, 15 (2015), <https://doi.org/10.1146/annurev-conmatphys-031214-014726>.
- [11] A. D. Luca and A. Scardicchio, Ergodicity breaking in a model showing many-body localization, *Europhysics Letters* **101**, 37003 (2013).
- [12] E. Levi, M. Heyl, I. Lesanovsky, and J. P. Garrahan, Robustness of many-body localization in the presence of dissipation, *Phys. Rev. Lett.* **116**, 237203 (2016).
- [13] A. P. Luca D'Alessio, Yariv Kafri and M. Rigol, From quantum chaos and eigenstate thermalization to statistical mechanics and thermodynamics, *Advances in Physics* **65**, 239 (2016), <https://doi.org/10.1080/00018732.2016.1198134>.
- [14] P. W. Anderson, Absence of diffusion in certain random lattices, *Phys. Rev.* **109**, 1492 (1958).
- [15] L. Fleishman and P. W. Anderson, Interactions and the anderson transition, *Phys. Rev. B* **21**, 2366 (1980).
- [16] A. M. Finkel'shtein, Influence of Coulomb interaction on the properties of disordered metals, *Soviet Journal of Experimental and Theoretical Physics* **57**, 97 (1983).
- [17] T. Giamarchi and H. J. Schulz, Anderson localization and interactions in one-dimensional metals, *Phys. Rev. B* **37**, 325 (1988).
- [18] B. L. Altshuler, Y. Gefen, A. Kamenev, and L. S. Levitov, Quasiparticle lifetime in a finite system: A nonperturbative approach, *Phys. Rev. Lett.* **78**, 2803 (1997).
- [19] I. V. Gornyi, A. D. Mirlin, and D. G. Polyakov, Interacting electrons in disordered wires: Anderson localization and low- t transport, *Phys. Rev. Lett.* **95**, 206603 (2005).
- [20] D. Basko, I. Aleiner, and B. Altshuler, Metal-insulator transition in a weakly interacting many-electron system with localized single-particle states, *Annals of Physics* **321**, 1126 (2006).
- [21] B. Bauer and C. Nayak, Area laws in a many-body localized state and its implications for topological order, *Journal of Statistical Mechanics: Theory and Experiment* **2013**, P09005 (2013).

- [22] M. Serbyn, Z. Papić, and D. A. Abanin, Universal slow growth of entanglement in interacting strongly disordered systems, *Phys. Rev. Lett.* **110**, 260601 (2013).
- [23] Y. Huang, Extensive entropy from unitary evolution, Preprints 10.20944/preprints202104.0254.v1 (2021).
- [24] D. A. Abanin, E. Altman, I. Bloch, and M. Serbyn, Colloquium: Many-body localization, thermalization, and entanglement, *Rev. Mod. Phys.* **91**, 021001 (2019).
- [25] P. Sierant and J. Zakrzewski, Many-body localization of bosons in optical lattices, *New Journal of Physics* **20**, 043032 (2018).
- [26] A. Lukin, M. Rispoli, R. Schittko, M. E. Tai, A. M. Kaufman, S. Choi, V. Khemani, J. Léonard, and M. Greiner, Probing entanglement in a many-body localized system, *Science* **364**, 256 (2019), <https://www.science.org/doi/pdf/10.1126/science.aau0818>.
- [27] Y. Bar Lev, G. Cohen, and D. R. Reichman, Absence of diffusion in an interacting system of spinless fermions on a one-dimensional disordered lattice, *Phys. Rev. Lett.* **114**, 100601 (2015).
- [28] M. Schreiber, S. S. Hodgman, P. Bordia, H. P. Lüschen, M. H. Fischer, R. Vosk, E. Altman, U. Schneider, and I. Bloch, Observation of many-body localization of interacting fermions in a quasirandom optical lattice, *Science* **349**, 842 (2015), <https://www.science.org/doi/pdf/10.1126/science.aaa7432>.
- [29] S. Bera, H. Schomerus, F. Heidrich-Meisner, and J. H. Bardarson, Many-body localization characterized from a one-particle perspective, *Phys. Rev. Lett.* **115**, 046603 (2015).
- [30] M. Serbyn, Z. Papić, and D. A. Abanin, Local conservation laws and the structure of the many-body localized states, *Phys. Rev. Lett.* **111**, 127201 (2013).
- [31] D. A. Huse, R. Nandkishore, and V. Oganesyan, Phenomenology of fully many-body-localized systems, *Phys. Rev. B* **90**, 174202 (2014).
- [32] A. Chandran, I. H. Kim, G. Vidal, and D. A. Abanin, Constructing local integrals of motion in the many-body localized phase, *Phys. Rev. B* **91**, 085425 (2015).
- [33] L. Rademaker and M. Ortuño, Explicit local integrals of motion for the many-body localized state, *Phys. Rev. Lett.* **116**, 010404 (2016).
- [34] S. J. Thomson and M. Schiró, Time evolution of many-body localized systems with the flow equation approach, *Phys. Rev. B* **97**, 060201 (2018).
- [35] D. Pekker, B. K. Clark, V. Oganesyan, and G. Refael, Fixed points of Wegner-Wilson flows and many-body localization, *Phys. Rev. Lett.* **119**, 075701 (2017).
- [36] R. Resta, Quantum-mechanical position operator in extended systems, *Phys. Rev. Lett.* **80**, 1800 (1998).
- [37] R. Resta and S. Sorella, Electron localization in the insulating state, *Phys. Rev. Lett.* **82**, 370 (1999).
- [38] I. Souza, T. Wilkens, and R. M. Martin, Polarization and localization in insulators: Generating function approach, *Phys. Rev. B* **62**, 1666 (2000).
- [39] R. Resta, Why are insulators insulating and metals conducting?, *Journal of Physics: Condensed Matter* **14**, R625 (2002).
- [40] X.-M. Lu and X. Wang, Operator quantum geometric tensor and quantum phase transitions, *Europhysics Letters* **91**, 30003 (2010).
- [41] E. Valença Ferreira de Aragão, D. Moreno, S. Battaglia, G. L. Bendazzoli, S. Evangelisti, T. Leininger, N. Suaud, and J. A. Berger, A simple position operator for periodic systems, *Phys. Rev. B* **99**, 205144 (2019).
- [42] B. Hetényi and B. Dóra, Quantum phase transitions from analysis of the polarization amplitude, *Phys. Rev. B* **99**, 085126 (2019).
- [43] B. Hetényi and S. m. c. Cengiz, Geometric cumulants associated with adiabatic cycles crossing degeneracy points: Application to finite size scaling of metal-insulator transitions in crystalline electronic systems, *Phys. Rev. B* **106**, 195151 (2022).
- [44] R. Resta, Electron localization in the quantum hall regime, *Phys. Rev. Lett.* **95**, 196805 (2005).
- [45] T. Wilkens and R. M. Martin, Quantum monte carlo study of the one-dimensional ionic hubbard model, *Phys. Rev. B* **63**, 235108 (2001).
- [46] T. Thonhauser and D. Vanderbilt, Insulator/Chern-insulator transition in the Haldane model, *Phys. Rev. B* **74**, 235111 (2006).
- [47] M. Filippone, P. W. Brouwer, J. Eisert, and F. von Oppen, Drude weight fluctuations in many-body localized systems, *Phys. Rev. B* **94**, 201112 (2016).
- [48] P. Sierant, A. Maksymov, M. Kuś, and J. Zakrzewski, Fidelity susceptibility in gaussian random ensembles, *Phys. Rev. E* **99**, 050102 (2019).
- [49] A. Maksymov, P. Sierant, and J. Zakrzewski, Energy level dynamics across the many-body localization transition, *Phys. Rev. B* **99**, 224202 (2019).
- [50] D. Sels and A. Polkovnikov, Dynamical obstruction to localization in a disordered spin chain, *Phys. Rev. E* **104**, 054105 (2021).
- [51] R. Resta, The insulating state of matter: a geometrical theory, *The European Physical Journal B* **79**, 121 (2011).
- [52] R. Resta, Geometry and topology in many-body physics (2020), arXiv:2006.15567 [cond-mat.str-el].
- [53] Q. Niu, D. J. Thouless, and Y.-S. Wu, Quantized hall conductance as a topological invariant, *Phys. Rev. B* **31**, 3372 (1985).
- [54] D. Banerjee, Topological aspects of the berry phase, *Fortschritte der Physik/Progress of Physics* **44**, 323 (1996), <https://onlinelibrary.wiley.com/doi/pdf/10.1002/prop.2190440403>.
- [55] L. Campos Venuti and P. Zanardi, Quantum critical scaling of the geometric tensors, *Phys. Rev. Lett.* **99**, 095701 (2007).
- [56] H. Watanabe, Insensitivity of bulk properties to the twisted boundary condition, *Phys. Rev. B* **98**, 155137 (2018).
- [57] S. S. Kondov, W. R. McGehee, W. Xu, and B. DeMarco, Disorder-induced localization in a strongly correlated atomic hubbard gas, *Phys. Rev. Lett.* **114**, 083002 (2015).
- [58] M. Serbyn, Z. Papić, and D. A. Abanin, Criterion for many-body localization-delocalization phase transition, *Phys. Rev. X* **5**, 041047 (2015).
- [59] R. Mondaini and M. Rigol, Many-body localization and thermalization in disordered hubbard chains, *Phys. Rev. A* **92**, 041601 (2015).
- [60] J. Chen, C. Chen, and X. Wang, Many-body localization transition in the disordered bose-hubbard chain (2023), arXiv:2104.08582 [cond-mat.dis-nn].
- [61] T. Ozawa and N. Goldman, Probing localization and quantum geometry by spectroscopy, *Phys. Rev. Res.* **1**, 032019 (2019).
- [62] E. J. Wilkens, G. Lawrence, A. Walsh, K. Morita, S. Simpson, C. Ritter, G. B. G. Stenning, A. M. Arevalo-

Lopez, and A. C. McLaughlin, Observation of an exotic insulator to insulator transition upon electron doping the mott insulator cemnaso, Nat. Comm. **14**, 7037 (2023).

Obtaining the Quantum Metric Without Full Diagonalization

Here we provide details for our algorithm to calculate the quantum metric without full diagonalizing the Hamiltonian. This method is faster and requires less memory as the all quantities can be stored as a sparse matrix. Take the Hamiltonian with twist boundary phases $\theta = (\theta_x, \theta_y, \theta_z)$ θ to be $H(\theta)$ and we target the quantum metric of the state $H(\theta)|\phi_0\rangle = E_0|\phi_0\rangle$. The quantum geometric tensor is given by

$$Q_{\mu\nu} = \sum_{m \neq 0} \frac{\langle \phi_0 | \partial_\mu H(\theta) | \phi_m \rangle \langle \phi_m | \partial_\nu H(\theta) | \phi_0 \rangle}{(E_m - E_0)^2} \quad (7)$$

where ∂_μ is the derivative with respect to the θ_μ . Note that $H(\theta) - E_0 = \sum_{m \neq 0} (E_m - E_0) |\phi_m\rangle \langle \phi_m|$, which implies $[H(\theta) - E_0]^{-2} = \sum_{m \neq 0} \frac{1}{(E_m - E_0)^2} |\phi_m\rangle \langle \phi_m|$ by the orthogonality of eigenstates. The quantum metric then becomes

$$Q_{\mu\nu} = \langle 0 | \partial_\mu H(\theta) [H(\theta) - E_0]^{-2} \partial_\nu H(\theta) | 0 \rangle \quad (8)$$

We can therefore calculate the quantum metric by obtaining only the state $|\phi_0\rangle$ and its energy E_0 . Since we want the state in the middle of the spectrum that corresponds to infinite temperature, we first obtain the largest and smallest energy states to shift the spectrum. Then the state of interest can be obtained by finding the eigenstate with energy closest to 0. We provide explicit MATLAB code in Table I that should be adaptable to other languages using standard libraries.

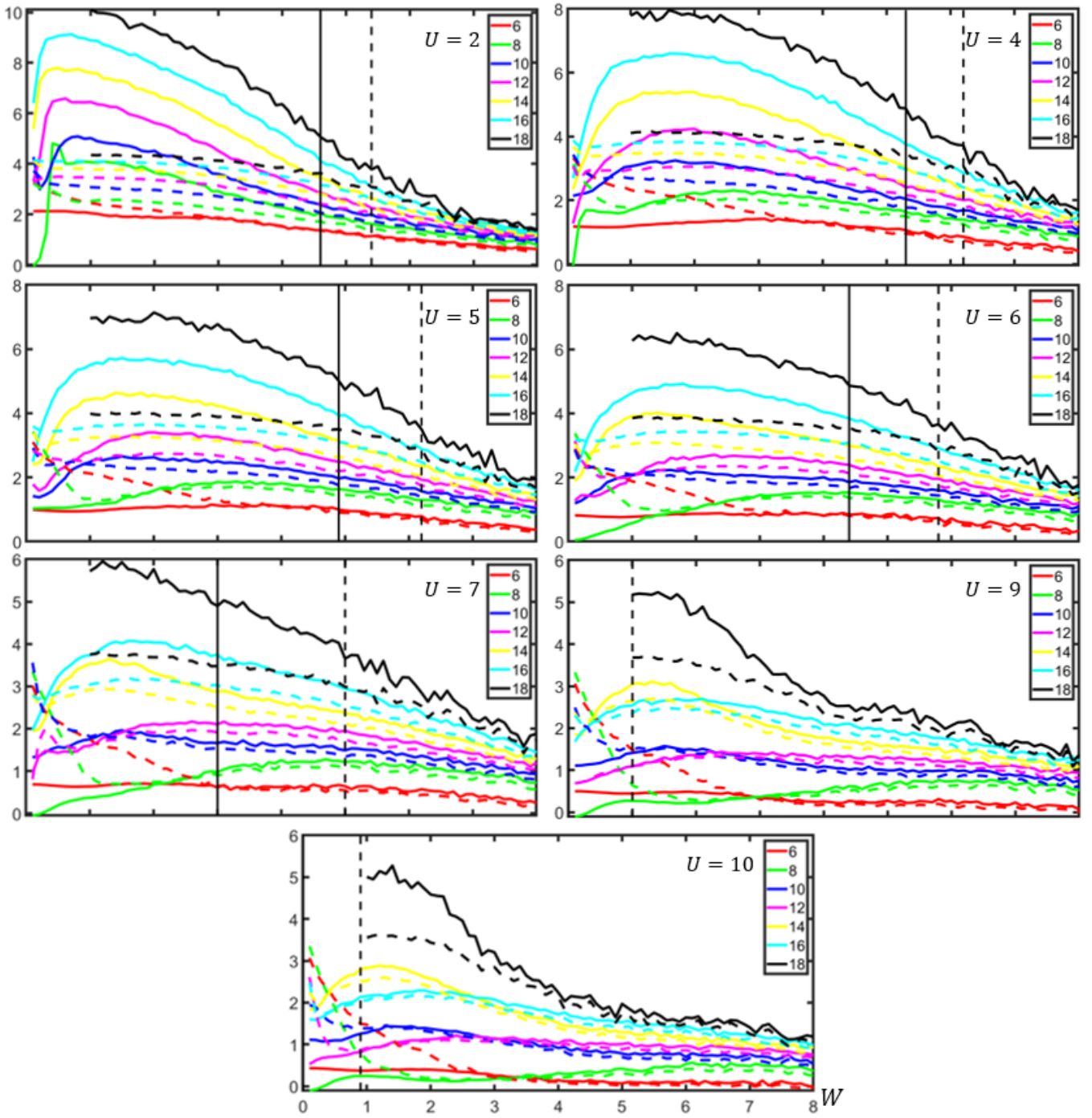


FIG. 5. Quantum metric $g_N = 4\pi^2 N g$ (solid) and localization length parameter $D_N = -N \ln |z_N|^2$ (dashed) versus disorder strength for different fixed interaction strengths U . The legend refers to the number of lattice sites in the chain L .

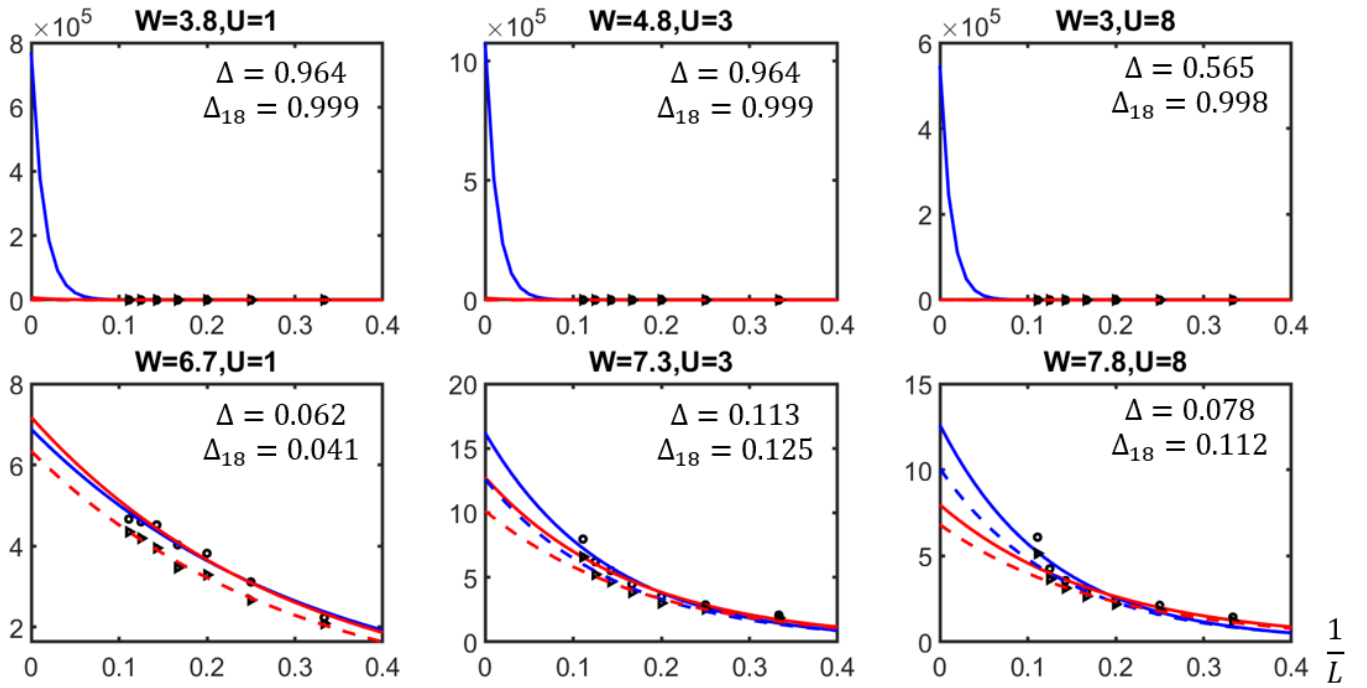


FIG. 6. Examples of thermodynamic limits for different parameters. The upper row is always in the ergodic regime while the lower is in the MBL. Black circles correspond to g_N while triangles correspond to D_N as obtained from taking the median over several disorder realizations. The solid line is the fit for g_N while the dashed is the fit for D_N . The blue coloring is with the inclusion of system size $L = 18$ while the red is with only system sizes up to $L = 16$.

Algorithm

H is the Hamiltonian

$numB$ is the size of the Hilbert space

$dH\nu$ and $dH\mu$ are $\partial_\nu H$ and $\partial_\mu H$.

E	<code>= eigs(H, 10, 'bothendsreal')</code>
$Eshift$	<code>= (max(E)+min(E))/2</code>
$eigvec, eigval$	<code>= eigs(H - Eshift*speye(numB),10, 'smallestabs')</code>
$E0, index0$	<code>= min(abs(diag(eigval)))</code>
$E0$	<code>= eigval(index0,index0)</code>
$\phi0$	<code>= eigvec(:,index0)</code>
$dH\nu\phi0$	<code>= dHnu*phi0</code>
$dH\mu\phi0$	<code>= dHmu*phi0</code>
$HE2dH\nu\phi0$	<code>= mldivide(((H-(Eshift + E0)*speye(numB))*(H-(Eshift+E0)*speye(numB))),dHnuphi0)</code>
Qxx	<code>= dHmu\phi0'*HE2dHnu\phi0</code>

TABLE I. Table: Algorithm for calculating the quantum metric without full diagonalization as implemented in MATLAB. This algorithm allows us to overcome system size limitations by diagonalizing only the extremal eigenvalue which can be obtained by various numerical methods such as Lanczos algorithm. The trade-off is we have to perform this partial diagonalization twice.

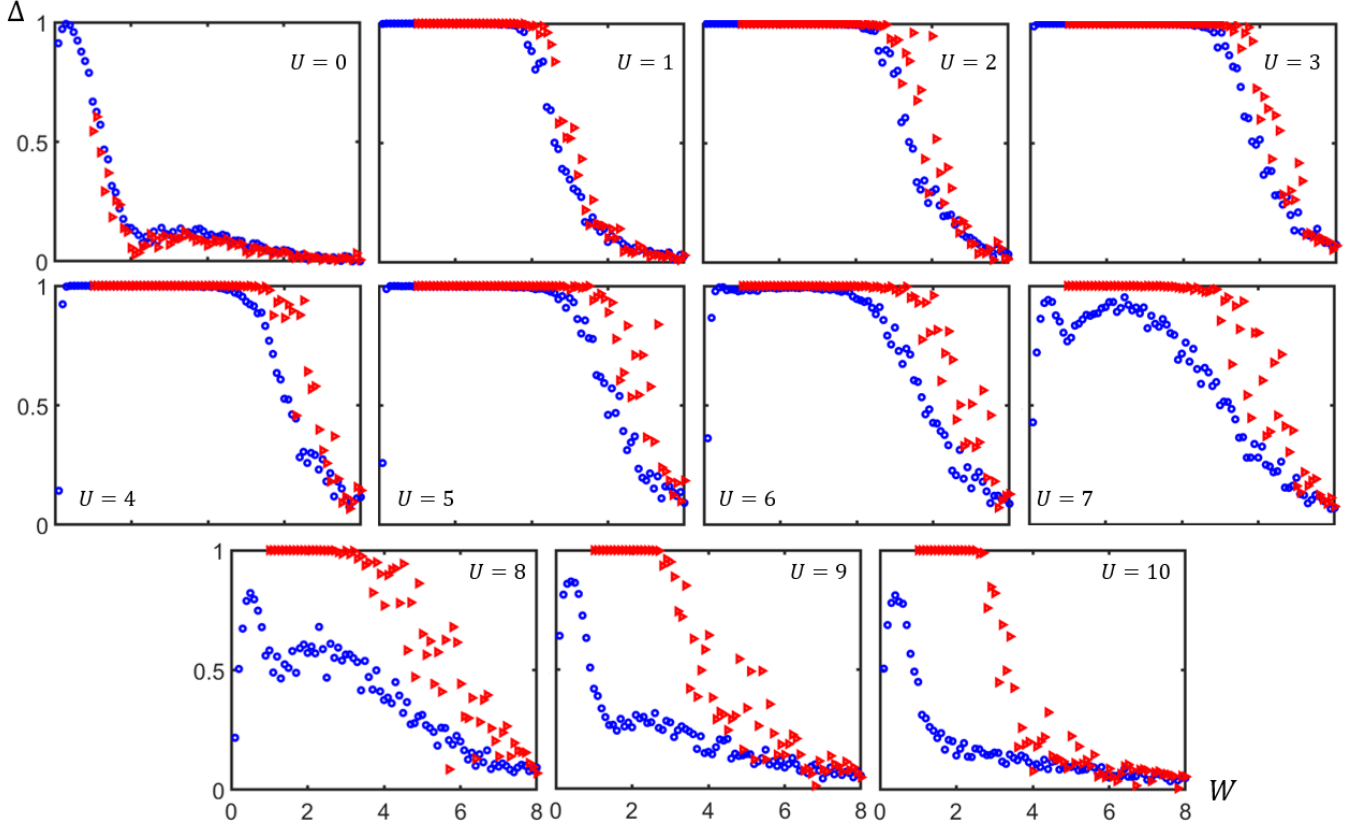


FIG. 7. Values of $\Delta = |D_\infty - g_\infty|/(D_\infty + g_\infty)$ as a function of disorder strength for fixed interaction U . This quantity is observed to be approximately 1 in the ergodic regime and goes to 0 in the MBL phase. The results for blue circles come from fitting to data from system sizes $L = 6$ to 16 while the red triangles include data from $L = 18$. In the paper we present results only from the blue circles due to the error in $L = 18$ from the lower number of samples considered.

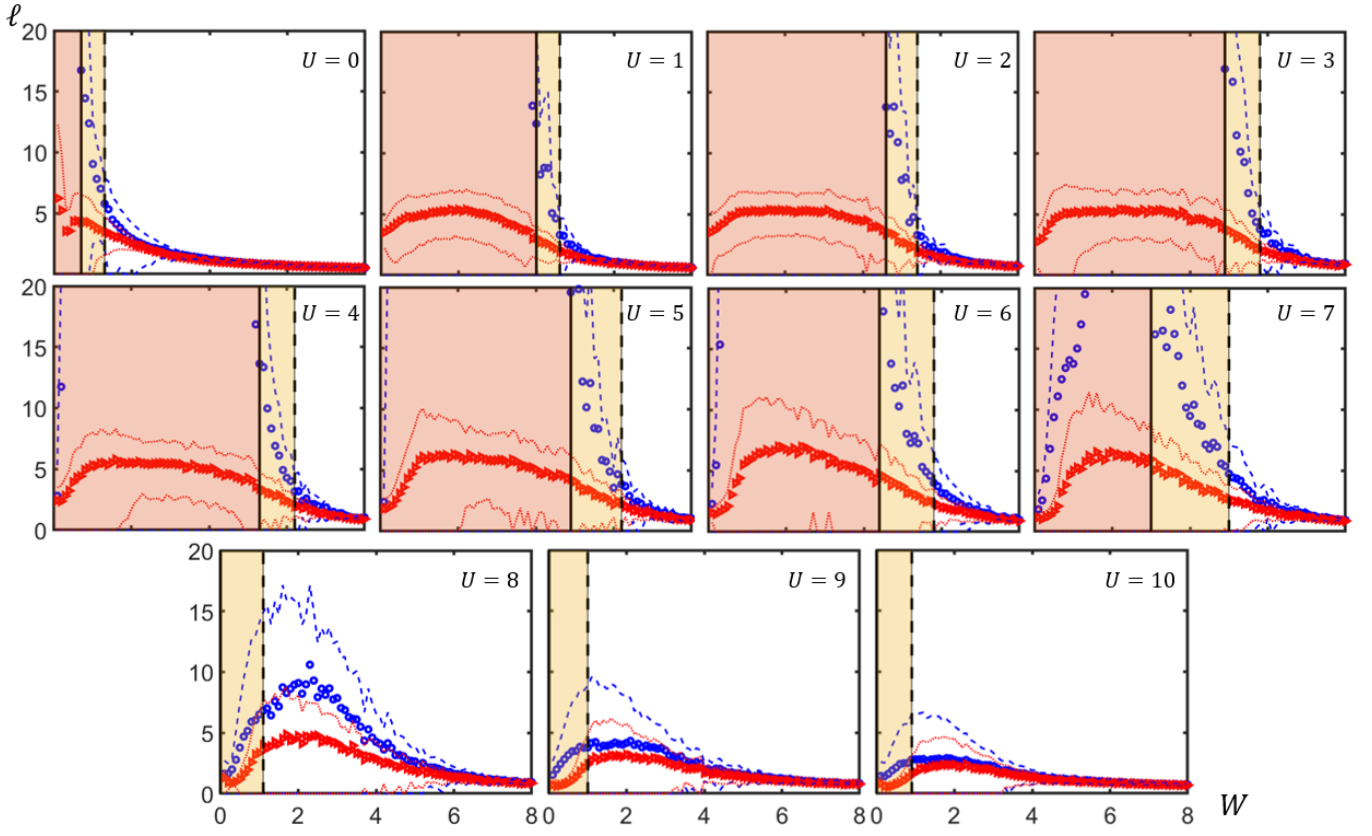


FIG. 8. Localization as a function of disorder for different interaction strengths. Localization lengths are extracted from the thermodynamic limit of the quantum metric g_N (blue circle) and D_N (red). The solid and dashed vertical lines correspond to the phase boundaries reported in Fig. 3. The regions where the system may still be ergodic is shaded in red or yellow as here the quantum metric is not related to the localization length with the red region being certainly in the ergodic phase while the yellow is within the transition region between ergodic and MBL.